Interleukin-22 promotes fibroblast- mediated wound repair in the skin

Heather M. McGee[2,1], **Barbara Schmidt**[1], **Carmen J. Booth**[3], **George D. Yancopoulos**[4], **David M. Valenzuela**[4], **Andrew J. Murphy**[4], **Sean Stevens**[4,5], **Richard A. Flavell**[2,#], and **Valerie Horsley**[1,#]

[1]Department of Molecular, Cell and Developmental Biology, Yale University

[2]Department of Immunobiology, Yale University

[3]Section of Comparative Medicine, Yale University

[4]Regeneron Pharmaceuticals, Inc., Tarrytown, NY

Abstract

Skin wound repair requires complex and highly coordinated interactions between keratinocytes, fibroblasts and immune cells to restore the epidermal barrier and tissue architecture after acute injury. The cytokine interleukin-22 (IL-22) mediates unidirectional signaling from immune cells to epithelial cells during injury of peripheral tissues such as the liver and colon, where IL-22 causes epithelial cells to produce anti-bacterial proteins, express mucins, and enhance epithelial regeneration. In this study, we use *IL-22*$^{-/-}$ mice to investigate the *in vivo* role for IL-22 in acute skin wounding. We find that *IL-22*$^{-/-}$ mice display major defects in the skin's dermal compartment after full thickness wounding. We find that IL-22 signaling is active in fibroblasts using *in vitro* assays with primary fibroblasts and that IL-22 directs extracellular matrix (ECM) gene expression as well as myofibroblast differentiation both *in vitro* and *in vivo*. These data define roles of IL-22 beyond epithelial crosstalk, and suggest that IL-22 plays a previously unidentified role in skin repair by mediating interactions between immune cells and fibroblasts.

Keywords

Interleukin 22; Wound Healing; Fibroblasts; extracellular matrix

Correspondence should be addressed to: Valerie Horsley, valerie.horsley@yale.edu, Dept. of Molecular, Cellular and Developmental Biology, Yale University, 219 Prospect St., Box 208103, New Haven, CT 06520, Tel #203-436-9126, Fax #203-432-6161 or Richard A. Flavell, richard.flavell@yale.edu, Howard Hughes Medical Institute and Dept. of Immunobiology, Yale University, 300 Cedar Street, Box 208011, New Haven, CT 06519, Tel # 203-737-2216, Fax # 203-737-2958.
#These laboratories contributed equally to this study.
5Current Address: Research AbLexis, LLC, 409 Illinois Street, San Francisco, CA 94158

Introduction

Breaches to epithelial barriers such as the skin result in an inflammatory response that prevents infection and augments tissue repair via the release of cytokines that signal between the immune system and cells in the damaged tissue (Barrientos *et al.*, 2008; Eming *et al.*, 2007). In the skin, wound repair requires interactions between keratinocytes, fibroblasts, immune cells and endothelial cells. Communication between these cells restores the epithelial barrier via keratinocyte proliferation and migration while reestablishing the dermal architecture through extracellular matrix production and myofibroblast-mediated wound contraction.

Members of the interleukin-10 (IL-10) cytokine family are soluble factors that orchestrate interactions between the immune system and peripheral tissues (Dumoutier *et al.*, 2001; Kotenko, 2002). One member of the IL-10 cytokine family, IL-22, is produced by both adaptive and innate lymphoid cells (Cella *et al.*, 2009; Cupedo *et al.*, 2009; Eyerich *et al.*, 2009; Goto *et al.*, 2009; Liang *et al.*, 2006; Martin *et al.*, 2009; Takatori *et al.*, 2009). IL-22 mediates its functions in tissues by binding to its heterodimeric receptor consisting of IL-10 receptorβ (IL-10Rβ) and IL-22 receptor α (IL-22Rα) and activating signaling pathways that stimulate STAT3 phosphorylation and nuclear translocation (Dumoutier *et al.*, 2001; Dumoutier *et al.*, 2003; Kotenko *et al.*, 2001; Lejeune *et al.*, 2002; Xie *et al.*, 2000). While IL-10Rβ is expressed ubiquitously on both immune cells and tissue specific cell types, IL-22RαEis thought to be exclusively expressed on epithelial cells, such as keratinocytes in the skin and hepatocytes in the liver (Dumoutier *et al.*, 2003; Radaeva *et al.*, 2004; Wolk *et al.*, 2004). The restriction of IL-22Rα expression allows IL-22 to mediate uni-directional signaling from the immune system to tissue-specific cells.

Many similarities can be made between the repair processes that occur in the skin and those that occur in other organs containing epithelium such as the thymus, lung, and the intestine, where IL-22 mediates signaling to epithelial cells (Dudakov *et al.*, 2012; Radaeva *et al.*, 2004; Sasaki *et al.*, 2011; Zenewicz *et al.*, 2007; Zenewicz *et al.*, 2008). In the skin, IL-22 is expressed after burn wounding (Sasaki *et al.*, 2011), elevated in human psoriasis patients (Lowes *et al.*, 2008) and promotes dermal inflammation (Ma *et al.*, 2008; Zhang *et al.*, 2012; Zheng *et al.*, 2007). *In vitro* studies have suggested that IL-22 signals to the epithelial keratinocytes of the skin to promote proliferation and migration while repressing keratinocyte differentiation (Boniface *et al.*, 2005; Wolk *et al.*, 2006); however, the function *of* IL-22 *in vivo* during acute skin wound healing has not been explored.

In this study, we investigated the role of IL-22 in a murine model of acute skin wounding. Wefind that *IL-22* mRNA is upregulated during the inflammatory response following tissue injury. Surprisingly, keratinocytes in the skin of *IL-22*$^{-/-}$ mice display only minor defects in their ability to repair the epithelial barrier during wound healing. However, *IL-22*$^{-/-}$ wounds exhibit severe defects in the dermal compartment due to deficiencies in fibroblast function. We show that IL-22-induced signaling in fibroblasts regulates extracellular matrix (ECM) production and myofibroblast differentiation during proper wound healing. Therefore, our results demonstrate that IL-22 mediates signaling beyond epithelial cells and is required for normal fibroblast function during skin wound repair.

RESULTS

IL-22 mRNA expression during acute skin wounding

To determine whether IL-22 might play a role in acute skin wounding, we analyzed the expression of *IL-22* and *IL-22Rα* mRNA in a murine model of full-thickness skin wounds. The dorsal skin of wild-type (WT) mice was wounded using 2 or 8mm skin punch biopsies as indicated. For each wound size, wounds were harvested during and after the inflammatory phase of wound healing as indicated by *CD45* mRNA and protein expression in 3 day skin wounds of 2mm biopsies (referred to as small wounds) and in 5 day skin wounds of 8mm biopsies (referred to as large wounds) (Figure 1A and data not shown) (Eming *et al.*, 2007). *IL-22* mRNA was not detected in unwounded skin (Figure 1B). However, *IL-22* mRNA was upregulated during the inflammatory phase of wound healing, and its expression returned to steady-state following inflammation (Figure 1B). In contrast, *IL-22Rα* mRNA expression increased only slightly during the inflammatory phase compared to unwounded skin, but its expression returned to baseline levels following inflammation (Figure 1C). These data are consistent with the induction of *IL-22* mRNA expression after infectious or injurious stimuli in the liver and colon (Radaeva *et al.*, 2004; Zenewicz *et al.*, 2007; Zenewicz *et al.*, 2008). Taken together, these data demonstrate that IL-22 signaling components are expressed in the skin during acute wound healing.

Delayed wound healing in *IL-22*$^{-/-}$ mice

Since *IL-22* mRNA expression is upregulated in the skin after wounding, we investigated if acute wound healing was defective in *IL-22*$^{-/-}$ mice. No overt skin defects were observed in *IL-22*$^{-/-}$ mice during development (data not shown) or in adult mice (Supplementary Figure 1A). To investigate whether IL-22 plays a role in wound healing *in vivo*, we generated small and large full-thickness wounds in the dorsal skin of sex-matched WT and *IL-22*$^{-/-}$ mice during the telogen phase of the hair cycle (Supplementary Figure 1A). Immune cell recruitment and blood vessel formation were similar between wounds of WT and *IL-22* null mice, as indicated by expression of CD45 and isolectin GS-IB4 (Tammela *et al.*, 2008) respectively (Supplementary Figures 2A and 2B).

Surprisingly, keratinocyte function during wound healing was not significantly impaired in *IL-22* null mice in this wound model as indicated by similar epidermal area (Supplementary Figure 1B), proliferation of keratinocytes in the leading edge (Supplementary Figures 1C and 1D), and rates of reepithelialization (Supplemental Figure 1E) as WT mice. In addition, induction of the antimicrobial protein, cathelicidin (Dorschner *et al.*, 2001), occurred normally in *IL-22* null wounds despite the ability of IL-22 to regulate antimicrobial gene expression (Liang et al., 2006) (Supplemental Figure 2C).

In contrast, a major difference in external wound area and the appearance of the dermal compartment was noted in both small and large wounds of *IL-22*$^{-/-}$ mice. In WT mice, the external area of small wounds was ~1.2×10^3 μm^2 at day 3 and it decreased to ~500 μm^2 by day 5. In contrast, the average external area of small wounds in *IL-22*$^{-/-}$ mice was ~2×10^3 μm^2 at day 3, and it decreased slightly to ~1.5×10^3 μm^2 at day 5 (Figure 2A). Morphometric analysis of hematoxylin and eosin-stained sections from 2mm or 8mm wounds of WT and

IL-$22^{-/-}$ mice post-injury revealed a striking defect in the dermis of IL-$22^{-/-}$ mice. The area underneath the wound bed referred to as wound bed area was decreased in both small and large wounds (Figure 2B). Furthermore, hematoxylin and eosin stained sections revealed alterations in the organization of the dermal compartment of both small and large wounds in IL-$22^{-/-}$ mice (Figure 2B and data not shown).

Defects in extracellular matrix production in *IL-22*$^{-/-}$ mice

To determine if the reduced wound bed area in IL-$22^{-/-}$ mice was due to defects in ECM production, we analyzed skin sections of WT and IL-$22^{-/-}$ mice using the histological stains Movat Pentachrome to reveal total collagen and Sirius Red to stain Collagen Type III. During the inflammatory phase of wound healing, collagen was localized adjacent to the wound bed and was decreased in IL-$22^{-/-}$ mice (Figure 3A). After inflammation, collagen localization in IL-$22^{-/-}$ wounds resembled that of WT wounds at day 3, suggesting a delay in collagen production in the absence of IL-22 (Figure 3A). Moreover, Sirius Red staining revealed that Collagen Type III fibers were disorganized in IL-$22^{-/-}$ mice at day 28 in the remodeling phase of wound healing.

To determine if the reduction in collagen protein content in IL-$22^{-/-}$ skin results from defects in the transcription of ECM genes, we analyzed *Fibronectin*, *Collagen Type IaI* and *Collagen Type IIIaI* mRNA expression from WT and IL-$22^{-/-}$ skin post-wounding (Figure 3B). Wound healing in WT mice was characterized by an initial upregulation of *Fibronectin* and *Collagen Type IIIaI* mRNAs during inflammation, but these gene products decreased following the inflammatory phase. In contrast, *Collagen Type IaI* mRNA levels increased and remained elevated during these timepoints in WT mice. Our data shows that the levels of *Fibronectin*, *Collagen Type IaI* and *Collagen Type IIIaI* were significantly reduced in IL-$22^{-/-}$ skin compared to WT skin (Figure 3B). Therefore, delayed wound healing in IL-$22^{-/-}$ mice is consistent with a delay in the expression of ECM genes during wound healing.

Considering that ECM components are produced by fibroblasts within the dermis, we hypothesized that fibroblast number or ECM production was decreased in IL-$22^{-/-}$ mice. To determine if IL-22 affects the number of fibroblasts, we isolated WT and IL-$22^{-/-}$ dermal cells from unwounded skins and from skins post-wounding. Using flow cytometry, we analyzed of the percentage of fibroblasts by staining dermal cells with an antibody against the fibroblast-specific protein ER-TR7 (Van Vliet *et al.*, 1984). We found no significant difference in the percentage of ER-TR7^{+} fibroblasts isolated from IL-$22^{-/-}$ wounds compared to WT wounds (Figure 3C).

To confirm that the dermal defects are due to an absence of IL-22 during dermal remodeling, we injected recombinant IL-22 intradermally into IL-$22^{-/-}$ wounds 3 days after wounding when the initial defects in the dermis are detected in IL-$22^{-/-}$ mice. The severe defect in collagen production in IL-$22^{-/-}$ mice is restored by intradermal IL-22 (Figure 3D). This result confirms that IL-22 is essential for proper dermal organization following wounding.

IL-22 activates extracellular matrix gene expression in fibroblasts

To determine whether IL-22 acts directly on fibroblasts during wound healing, TaqMan real-time PCR was used to measure *IL-22Rα* expression in FACS-purified murine keratinocytes, naïve CD4+CD25−CD44−CD62L+ T cells and purified dermal fibroblasts (Festa et al., 2011; Kunz et al. 2006). We used real time PCR to determine the purity of the isolated keratinocyte and fibroblast populations based on *K14* and *vimentin* mRNA expression (Figure S3B). As expected, *IL-22Rα* mRNA was not detected in naïve T cells, but was expressed in keratinocytes (Kunz *et al.*, 2006)(Figure 4A). Surprisingly, *IL-22Rα*mRNA was also expressed in fibroblasts. This expression was confirmed by immunostaining with antibodies against ER-TR7 and IL-22Rα in skin sections (Figure 4B). Specificity of the IL-22Rα staining was confirmed by immunostaining with rabbit isotype control antibodies (Figure S3C).

To determine if IL-22 can activate signaling downstream from IL-22Rα in fibroblasts, we analyzed STAT3 phosphorylation since IL-22 induces STAT3 phosphorylation and nuclear translocation in other cell types (Lejeune *et al.*, 2002). Primary fibroblasts were serum starved and then stimulated for 20 minutes with vehicle, Oncostatin M, which activates STAT3 in fibroblasts (Snyder *et al.*, 2008), or recombinant IL-22. Immunostaining of fibroblasts with antibodies against phosphorylated STAT3 (STAT3-P) revealed activation of STAT3 following stimulation with either OSM or IL-22 (Figure 4C). Western analysis of fibroblast cell lysates following OSM or IL-22 stimulation confirmed that IL-22 stimulates phosphorylation of STAT3 in fibroblasts (Figure 4D). Taken together, these data demonstrate that fibroblasts express functional IL-22Rα and that IL-22/IL-22Rα signaling is sufficient to activate STAT3-P in fibroblasts.

To determine whether IL-22 can directly stimulate the production of the ECM components in fibroblasts, primary cultured dermal fibroblasts isolated from WT or *IL-22* null mice were stimulated with recombinant IL-22 for 48 hours. We analyzed mRNA expression by real-time PCR. IL-22 induced a dose-dependent increase in mRNA expression of *Fibronectin*, *Collagen Type IαI* and *Collagen Type IIIαI*, but not *Integrin α5* or *Metalloproteinase 9* (*MMP9*), which mediate adhesion to or degradation of ECM molecules, respectively (Figure 4E) (Liu *et al.*, 2010; Sawicki *et al.*, 2005). Since *IL-22−/−* fibroblasts also induce ECM genes in response to IL-22, no intrinsic defects exist in the fibroblasts from *IL-22−/−* mice. These changes in gene expression were confirmed by Western analysis of fibronectin protein expression after IL-22 stimulation (Figure 4F). Taken together, these data suggest that IL-22 signaling in fibroblasts can directly induce the expression of ECM components.

IL-22 activates myofibroblast differentiation

Since *IL-22−/−* mice display defects in wound contraction and ECM production following wounding, we hypothesized that IL-22 may influence the differentiation of dermal myofibroblasts, which contract wounds and produce ECM during wound healing (Montesano and Orci, 1988). Myofibroblasts are identified by their characteristic expression of α-smooth muscle actin (α-SMA) (Darby *et al.*, 1990). To determine if the skin of *IL-22−/−* mice displays a reduction in the number of α-SMA+ myofibroblasts, we investigated whether the number of α-SMA+ fibroblasts was altered during wound healing

in the absence of IL-22. Immunostaining of WT and *IL-22*$^{-/-}$ wounds after wounding revealed a reduction in the number of α-SMA^{+} cells in the dermis of small and large *IL-22*$^{-/-}$ wounds compared to WT wounds (Figure 5A and data not shown). In addition, we isolated unwounded skin and day 3 wounded skin from WT and *IL-22*$^{-/-}$ mice and measured *α-SMA* mRNA expression via real-time PCR. While *α-SMA* mRNA expression increased in response to wounding in both WT and *IL-22*$^{-/-}$ mice, *α-SMA* mRNA expression was significantly reduced in wounds from *IL-22* null mice compared to WT wounds (Figure 5B). These data suggest there was a reduction in the number of myofibroblasts in the absence of IL-22.

Since the reduced number of α-SMA^{+} fibroblasts could be due to alterations in the differentiation of fibroblasts into myofibroblasts (Barisic-Dujmovic *et al.*, 2010), we investigated whether IL-22 was sufficient to induce myofibroblast differentiation. Primary dermal fibroblasts from WT or *IL-22* null mice were treated *in vitro* with recombinant IL-22 for 48 hours and *α-SMA* mRNA and protein expression was quantified. Real-time PCR analysis revealed a nine-fold increase in *α-SMA* mRNA expression after the addition of IL-22 in fibroblasts from both WT or *IL-22*$^{-/-}$ mice (Figure 5C). In addition, WT cultures displayed an increase in α-SMA protein as shown via Western blotting (Figure 5D). Taken together, these data suggest that IL-22 promotes myofibroblast differentiation and function in the skin following wounding. These data suggest that the lack of myofibroblasts is most likely responsible for the dermal remodeling defects in *IL-22* null mice.

Discussion

Given the essential functions of epithelia to protect mammalian tissues from the external environment, highly coordinated mechanisms between multiple cell types have evolved to repair epithelial tissue damage. The recruitment of immune cells following acute skin injury is essential for multiple stages of wound healing including keratinocyte reepithelialization, extracellular matrix deposition, granulation tissue remodeling and wound contraction by fibroblasts (Eming *et al.*, 2007). While extensive research has focused on cytokines and growth factors that mediate keratinocyte reepithelialization (Gurtner, 2008), very little is known about the signals that mediate cross-talk between immune cells and fibroblasts. Here we identify IL-22 as an essential signal that mediates communication between immune cells and fibroblasts in the skin.

Several studies have linked IL-22 to inflammatory conditions in tissues containing epithelial cells such as the thymus, the colon, and the skin (Kagami *et al.*, 2010; Sekikawa *et al.*, 2010; Yamamoto-Furusho *et al.*, 2010; Zenewicz *et al.*, 2008; Mizoguchi, et al 2012). *In vitro* studies have suggested that IL-22 induces keratinocyte proliferation and migration while inhibiting keratinocyte differentiation (Boniface *et al.*, 2005; Wolk *et al.*, 2006; Zheng *et al.*, 2007). Our data suggest that the loss of IL-22 alone does not cause major defects in early events involved in skin wound healing such as immune cell recruitment or blood vessel formation. Future experiments examining specific immune cell subsets, blood vessel architecture or keratinocyte function in the absence of IL-22 may reveal functions for this cytokine in additional aspects of skin wound healing. Furthermore, our experimental system did not detect defects in keratinocyte function during wounding *in vivo,* suggesting that

additional signaling molecules such as FGF7 and EGF (Werner and Grose, 2003) may compensate for a loss of IL-22 in the skin. Wound models that challenge the wound epidermis, such as with a stinted wound technique, may reveal a role for IL-22 in keratinocyte function.

Interestingly, our study uncovered a role for IL-22 in directing fibroblast function during skin wound repair. Fibroblasts have several functions that are defective in *IL-22⁻/⁻* mice, leading to abnormal granulation tissue formation, extracellular matrix protein production and wound contraction. These defects are likely due to direct action of IL-22 on fibroblasts since primary dermal fibroblasts express IL-22Rα and IL-22 can induce STAT3 phosphorylation in dermal fibroblasts downstream of the IL-22Rα. Our data show that IL-22 directly stimulates, extracellular matrix gene expression in primary dermal fibroblasts *in vitro* and that *IL-22⁻/⁻* mice lack, extracellular matrix components. Future studies will focus on whether IL-22 also acts on mesechymal cells in the other organs during acute regeneration.

Furthermore, the defects in ECM production may be linked to our finding that IL-22 promotes myofibroblast differentiation. Since the number of myofibroblasts is proportional to the rate of wound contraction and the amount of ECM produced (Gabbiani *et al.*, 1976), the defects in wound contraction and the delay in ECM production in *IL-22⁻/⁻* mice is likely due to a reduced number of α-SMA⁺ myofibroblasts in the wound bed. To our knowledge, this study illustrates a role for IL-22 on mesenchymal cells during cutaneous wound healing that is previously unreported. These data change the paradigm of IL-10 family cytokines as mediators of epithelial cell biology, showing that IL-22 also plays a key role mediating immune cell-stromal cell interactions during tissue repair.

IL-22 signaling may directly or indirectly stimulate the expression of ECM genes. Although IL-22 can signal via Jak/STAT, MAPK and Akt pathways (Lejeune 2002), the majority of the effects of IL-22 on epithelial cells have been linked to STAT3. Our work highlights a role for IL-22-induced STAT3 phosphorylation in dermal fibroblasts. Therefore, it is possible that IL-22 signaling directly activates the promoters of *Fibronectin*, *Collagen IIIαI* and *Collgen IαI* through STAT3 activation. Alternatively, it is posssible that IL-22 indirectly regulates ECM production by regulating myofibroblast differentiation.

Although IL-22 has been highlighted for its ability to protect epithelial cells in the liver and colon during inflammation, it also has been suggested to play a pathogenic role in psoriasis and collagen-induced arthritis (Geboes *et al.*, 2009; Kagami *et al.*, 2010; Lowes *et al.*, 2008; Wolk *et al.*, 2006). The results presented here could help explain some aspects of IL-22's pathogenicity, since IL-22 may act on fibroblast-like chondrocytes in the joints and fibroblasts in the skin to induce excessive collagen production in patients with rheumatoid arthritis or psoriasis, respectively (Koivukangas *et al.*, 1995; Steenvoorden *et al.*, 2006). In fact, IL-22 was recently shown to worsen synovitis by inducing the production of RANKL from synovial fibroblasts and therefore indirectly promoting osteoclastogenesis (Kim *et al.*, 2011). IL-22 was also shown to play a role in the pathogenesis of systemic sclerosis, which is consistent with our data (Truchetet *et al.*, 2011).

While normal levels and kinetics of IL-22 can enhance wound healing by inducing myofibroblast differentiation and ECM production, these physiologic processes may become pathogenic if excessive ECM production destroys normal tissue architecture and interferes with organ function (Jun and Lau, 2010a, b). Therefore, further studies on the role of IL-22 in conditions characterized by abnormal wound healing, such hypertrophic scarring and fibrotic diseases, will clarify the role of IL-22 in the pathogenesis of diseases characterized by defects in fibroblast-mediated tissue repair (Kong *et al.*, 2012).

MATERIALS AND METHODS

Mice

IL-22$^{-/-}$ mice were generated by using the VelociGene© method (VelociGene Allele Identification Number: VG204) in collaboration with Regeneron Pharmaceuticals (Valenzuela *et al.*, 2003). *K14*-H2BGFP mice were described previously (Tumbar *et al.*, 2004). For wounding studies, 7–8 week old male mice were used during the telogen phase of the hair cycle. Littermates and C57BL/6 (B6) mice were used as WT controls. A maximum of 4 wounds were made on the dorsal skin of each mouse. All animal care and experimental procedures were approved by the Yale University Animal Resource Center and were conducted in accord with requirements approved by the Institutional Animal Care and Use Committee of Yale University.

Skin Wounding and morphogenetic measurements

WT and *IL-22*$^{-/-}$ mice were anesthetized with isofluorane and full-thickness wounds were made on shaved dorsal skins using sterile dermal biopsy punches, 2mm, 4mm and 8mm as indicated (Accuderm). Wounds were air-exposed throughout the healing process. Images of the external appearance of the wounds was taken and the area of wound was measured using ImageJ software.

To measure histological characteristics of wounds, each wound was embedded and sectioned through its entirety. Sections from the middle of the wound, as indicated by the largest length of hyperproliferative epidermis, were used for all analyses. We determined the percentage of epidermal reepithelialization by measuring the total length of the hyperproliferative keratinocyte region and dividing by the total wound length (the sum of the lengths of the epithelium and unepithelialized dermis) (Qiu *et al.*, 2003). The maximal rate of wound closure was calculated using linear regression of the epithelialization data.

For rescue experiments, 20μL PBS or recombinant IL-22 (25ng/mL, R&D Systems) was injected intradermally at day 3 post-injury. The wound bed area was determined at indicated timepoints after wounding using Image J software.

For FACS, RNA and protein analysis, a circular area around 1mm larger than the wound was isolated at indicated timepoints in order to ensure that activated dermal fibroblasts in the wound margins were included.

Gene Expression Analysis

Quantitative real time PCR was performed as previously described (Horsley *et al.*, 2008; O'Connor *etal.*, 2009). The following accesion numbers were used for the Taqman primers: Mm00444241_m1 (*IL-22*) and Mm00663697_m1 (*IL-22Rα*). For quantitative PCR using SYBR green, the following primers were used: β-actin For 5′-ATC AAG ATC ATT GCT CCT CCT GAG-3′, Rev 5′-CTG CTT GCT GAT CCA CAT CTG-3′; Fibronectin For: 5′-CTA CCC TGC AGC CTC TGC GC-3′, Rev: 5′-TCA CCT CCC TGG CTC GGT CG-3′; Collagen IIIαI For: 5′-CTG GTC CTG TTG GTC CAT CT-3′, Rev: 5′-CTT CTC CAG CGG TAC CAG AG-3′; Collagen IαI For: 5′-ACG TCC TGG TGA AGT TGG TC-3′, Rev: 5′-TCC AGC AAT ACC CTG AGG TC-3′; MMP-9 For: 5′-ATC CCC AGA GCG TCA TTC GCG-3′, MMP-9 Rev: 5′-CAC GTA GCC CAC GTC GTC CAC-3′; α-SMA For: 5′-GTC CCA GAC ATC AGG GAG TAA-3′, Rev: 5′-TCG GAT ACT TCA GCG TCA GGA-3′; CD45 For: 5′-TAC GCA AAG CAC GGC CTG GG-3′, Rev: 5′-CTC CGG GGT TCC CAC CCC TC-3′; Vimentin For: 5′-CAG GGC AGC AGT GAG GTC-3′, Rev: 5′-TCC TCG AGC AGC AGA ACA AAA TCC-3′.

Dermal Fibroblast Isolation and IL-22 stimulation

Primary dermal fibroblasts were isolated from 8–12 week old mice using either Collagenase 1A (2.5mg/mL, Sigma) and DNaseI (62.5U/mL, Sigma) digestion or tail skin explant cultures. Following skin digestion, isolated cells were centrifuged after filtering and plated with high glucose DMEM (GIBCO) containing 10% FBS and 1% Penicillin/Streptomycin/ Amphotericin. Fibroblasts were grown to 85% confluence and recombinant IL-22 (R&D Systems) was added at indicated doses (10ng/mL or 20ng/mL) for 48 hours. Cells were harvested in Trizol for RNA extraction and cell lysates were harvested in RIPA buffer for Western analysis.

Isolation, culture and analysis of primary fibroblasts

Primary dermal fibroblasts were isolated from the wounded skin of 12 week old mice using Collagenase 1A (2.5mg/mL, Sigma) and DNaseI (62.5U/mL, Sigma) digestion. After filtering the digested tissue with $70\mu m^2$ mesh, cells were centrifuged and if cultured, plated in DMEM media containing glucose, 10% FBS and 1% Pen/Step/Amphotericin. For FACS analysis, freshly isolated cells were fixed, permeablized, and stained with rat α-ER-TR7 (1:250, Novus Biologicals) and Alexa 488 conjugated α-rabbit IgG (1:250, Invitrogen). Samples were analyzed on a FACS Aria and analyzed with FlowJo software.

Western blotting

To collect protein lysates from wounds *in vivo*, wounded skin was isolated and flash frozen in liquid N_2. Skin was minced and added to RIPA buffer (50mM Tris, 150mM NaCl, 0.1% SDS, 0.5% Na Deoxycholate, 1% NP-40) containing protease inhibitors (Roche). Tissue was homogenized, sonicated for 10 min and frozen at −80°C. To collect protein lysates from cell culture, cells were washed 1x with PBS (GIBCO) and then lysed with RIPA buffer.

Total protein was measured via Bradford assay and 10μg of protein was run on 4–20% Tris-Glycine gels (Invitrogen) before being transferred to nitrocellulose membranes. Membranes

were blocked with blocking buffer (5% non-fat dry milk, 10mM Tris, 100mM NaCl, 0.1% Tween-20) andprobed with the following primary antibodies: Rabbit polyclonal α-STAT3 (1:1000, Cell Signaling), murine monoclonal α-STAT3-P (1:1000 Cell Signaling), murine monoclonal α-Fibronectin (Calbiochem), and goat polyclonal α-alpha-SMA (Sigma), and murine monoclonal α-β-actin (1:20,000, Sigma) and secondary antibodies (1:5000, peroxidase-conjugated α-mouse IgG, α-rabbit IgG, and α-goat IgG). Western blots were visualized via chemiluminescence with the ECL Plus Detection System (Amersham).

Cell Sorting

To purify keratinocytes from mouse skin, *K14-H2BGFP* mice were shaved and dorsal skins were removed. The dermal side of skin was scraped to remove fat and floated on 0.25% trypsin overnight at 4°C. To release epidermal cells, the dorsal side of the skin was scraped, cells were filtered, washed in PBS and resuspended in PBS + 3% Serum + 1% Penicillin/Streptomycin/Amphotericin containing 503g/mL DNaseI. Cells were stained with propridium iodide and α-CD49f-PE (1:75; BD Biosciences) and CD49f$^+$, GFP$^+$, PI$^-$ keratinocytes were purified via FACS.

To purify naïve CD4$^+$ T cells from spleens, splenocytes were isolated from 6–8 week old C57BL/6 mice and a single cell suspension was treated with RBC lysis buffer. Cells were enriched for CD4$^+$ cells (L3T4 microbeads and MACS columns, Miltenyi Biotech). CD4$^+$CD25$^-$CD44$^-$CD62L$^+$ cells were purified by cell sorting on a FACS Vantage sorter with FITC–conjugated α-CD44, PE-conjugated α-CD25, APC-conjugated α-CD4, and PECy7-conjugated α-CD62L (all from BD Pharmingen). Sorted cell purity was >97%.

Histological Stains and Immunofluorescence

Wounded dorsal skins were mounted in O.C.T. compound (Tissue-Tek) on dry ice and cryosectioned for histological staining or immunostaining with indicated antibodies. For Movat Pentachrome and Sirius Red stains, skins were fixed in 10% Formalin-Buffered Saline, embedded in paraffin, sectioned through the entire length of the wound and stained. Trichrome staining was performed using Masson's trichrome stain kit according to the manufacturer's protocol (Polysciences, Inc).

Immunostaining was performed as described previously (Festa *et al.*, 2011). Briefly, tissue sections were fixed with 4% Formaldehyde and blocked with PBS containing 0.02% Gelatin, 0.25% Triton-X, 1% BSA plus normal goat and donkey serum. When applicable, the M.O.M. kit (Vector labs) was used to prevent non-specific binding of mouse antibodies. Slides were stained with rat polyclonal α-ER-TR7 (1:250, Novus Biologcials), rabbit polyclonal N-terminal α-IL-22R (1:250, QED Biosciences), rabbit polyclonal α-phospho-STAT3 (1:100, Cell Signaling), murine monoclonal α-SMA (1:250, Thermo Scientific), rabbit polyclonal α-Ki67 (1:300, Leica Microsystems), rat monoclonal CD45-PE-Cy7 (1:500, eBioscience), rabbit polyclonal cathelicidin (1:300, Novus Biologicals), or Isolectin GS-IB4 Alexa 488-conjugated (1:100, Invitrogen) overnight at 4°C, and then with required secondary antibodies (1:250).

Immunofluorescent staining of fibroblasts was performed on micro-coverslips in 6-well tissue culture plates. Cells were serum-starved for 24 hours and then treated with 25ng/mL recombinant Oncostatin M (R&D Systems) or 25ng/mL recombinant IL-22 (R&D Systems) for 20 minutes. Cells were washed and fixed in 4% formaldehyde before being stained with murine monoclonal α-STAT3-P (1:100, Cell Signaling). Image acqustiion was performed using a Zeiss confocal microscope or an upright Zeiss microscope with Axiovision software.

Statistical Analysis

To determine significance between groups, comparisons were made using student's t-tests. Analyses of multiple groups were performed using One-Way ANOVA with Bonferroni's posttest with GraphPad Prism version for Macintosh (GraphPad Software). For all statistical tests, the 0.05 level of confidence was accepted for statistical significance.

Supplementary Material

Refer to Web version on PubMed Central for supplementary material.

Acknowledgments

References

Barisic-Dujmovic T, Boban I, Clark SH. Fibroblasts/myofibroblasts that participate in cutaneous wound healing are not derived from circulating progenitor cells. J Cell Physiol. 2010; 222:703–12. [PubMed: 20020505]

Barrientos S, Stojadinovic O, Golinko MS, Brem H, Tomic-Canic M. Growth factors and cytokines in wound healing. Wound Repair Regen. 2008; 16:585–601. [PubMed: 19128254]

Boniface K, Bernard FX, Garcia M, Gurney AL, Lecron JC, Morel F. IL-22 inhibits epidermal differentiation and induces proinflammatory gene expression and migration of human keratinocytes. J Immunol. 2005; 174:3695–702. [PubMed: 15749908]

Cella M, Fuchs A, Vermi W, Facchetti F, Otero K, Lennerz JK, et al. A human natural killer cell subset provides an innate source of IL-22 for mucosal immunity. Nature. 2009; 457:722–5. [PubMed: 18978771]

Cupedo T, Crellin NK, Papazian N, Rombouts EJ, Weijer K, Grogan JL, et al. Human fetal lymphoid tissue-inducer cells are interleukin 17-producing precursors to RORC+ CD127+ natural killer-like cells. Nat Immunol. 2009; 10:66–74. [PubMed: 19029905]

Darby I, Skalli O, Gabbiani G. Alpha-smooth muscle actin is transiently expressed by myofibroblasts during experimental wound healing. Lab Invest. 1990; 63:21–9. [PubMed: 2197503]

Dorschner RA, Pestonjamasp VK, Tamakuwala S, Ohtake T, Rudisill J, Nizet V, et al. Cutaneous injury induces the release of cathelicidin anti-microbial peptides active against group A Streptococcus. J Invest Dermatol. 2001; 117:91–7. [PubMed: 11442754]

Dudakov JA, Hanash AM, Jenq RR, Young LF, Ghosh A, Singer NV, et al. Interleukin-22 drives endogenous thymic regeneration in mice. Science. 2012; 336:91–5. [PubMed: 22383805]

Dumoutier L, Leemans C, Lejeune D, Kotenko SV, Renauld JC. Cutting edge: STAT activation by IL-19, IL-20 and mda-7 through IL-20 receptor complexes of two types. J Immunol. 2001; 167:3545–9. [PubMed: 11564763]

Dumoutier L, Lejeune D, Hor S, Fickenscher H, Renauld JC. Cloning of a new type II cytokine receptor activating signal transducer and activator of transcription (STAT)1, STAT2 and STAT3. Biochem J. 2003; 370:391–6. [PubMed: 12521379]

Eming SA, Krieg T, Davidson JM. Inflammation in wound repair: molecular and cellular mechanisms. J Invest Dermatol. 2007; 127:514–25. [PubMed: 17299434]

Eyerich S, Eyerich K, Pennino D, Carbone T, Nasorri F, Pallotta S, et al. Th22 cells represent a distinct human T cell subset involved in epidermal immunity and remodeling. J Clin Invest. 2009; 119:3573–85. [PubMed: 19920355]

Festa E, Fretz J, Berry R, Schmidt B, Rodeheffer M, Horowitz M, et al. Adipocyte lineage cells contribute to the skin stem cell niche to drive hair cycling. Cell. 2011; 146:761–71. [PubMed: 21884937]

Gabbiani G, Le Lous M, Bailey AJ, Bazin S, Delaunay A. Collagen and myofibroblasts of granulation tissue. A chemical, ultrastructural and immunologic study. Virchows Arch B Cell Pathol. 1976; 21:133–45. [PubMed: 822577]

Geboes L, Dumoutier L, Kelchtermans H, Schurgers E, Mitera T, Renauld JC, et al. Proinflammatory role of the Th17 cytokine interleukin-22 in collagen-induced arthritis in C57BL/6 mice. Arthritis Rheum. 2009; 60:390–5. [PubMed: 19180498]

Goto M, Murakawa M, Kadoshima-Yamaoka K, Tanaka Y, Nagahira K, Fukuda Y, et al. Murine NKT cells produce Th17 cytokine interleukin-22. Cell Immunol. 2009; 254:81–4. [PubMed: 19010461]

Horsley V, Aliprantis AO, Polak L, Glimcher LH, Fuchs E. NFATc1 balances quiescence and proliferation of skin stem cells. Cell. 2008; 132:299–310. [PubMed: 18243104]

Jun JI, Lau LF. Cellular senescence controls fibrosis in wound healing. Aging (Albany NY). 2010a; 2:627–31. [PubMed: 20930261]

Jun JI, Lau LF. The matricellular protein CCN1 induces fibroblast senescence and restricts fibrosis in cutaneous wound healing. Nat Cell Biol. 2010b; 12:676–85. [PubMed: 20526329]

Kagami S, Rizzo HL, Lee JJ, Koguchi Y, Blauvelt A. Circulating Th17, Th22, and Th1 cells are increased in psoriasis. J Invest Dermatol. 2010; 130:1373–83. [PubMed: 20032993]

Kim KW, Kim HR, Park JY, Park JS, Oh HJ, Woo YJ, et al. IL-22 promotes osteoclastogenesis in rheumatoid arthritis through induction of RANKL in human synovial fibroblasts. Arthritis Rheum. 2011

Koivukangas V, Kallionen M, Karvonen J, Autio-Harmainen H, Risteli J, Risteli L, et al. Increased collagen synthesis in psoriasis in vivo. Arch Dermatol Res. 1995; 287:171–5. [PubMed: 7763089]

Kong X, Feng D, Wang H, Hong F, Bertola A, Wang FS, et al. Interleukin-22 induces hepatic stellate cell senescence and restricts liver fibrosis. Hepatology. 2012

Kotenko SV. The family of IL-10-related cytokines and their receptors: related, but to what extent? Cytokine Growth Factor Rev. 2002; 13:223–40. [PubMed: 12486876]

Kotenko SV, Izotova LS, Mirochnitchenko OV, Esterova E, Dickensheets H, Donnelly RP, et al. Identification of the functional interleukin-22 (IL-22) receptor complex: the IL-10R2 chain (IL-10Rbeta) is a common chain of both the IL-10 and IL-22 (IL-10-related T cell-derived inducible factor, IL-TIF) receptor complexes. J Biol Chem. 2001; 276:2725–32. [PubMed: 11035029]

Kunz S, Wolk K, Witte E, Witte K, Doecke WD, Volk HD, et al. Interleukin (IL)-19, IL-20 and IL-24 are produced by and act on keratinocytes and are distinct from classical ILs. Exp Dermatol. 2006; 15:991–1004. [PubMed: 17083366]

Lejeune D, Dumoutier L, Constantinescu S, Kruijer W, Schuringa JJ, Renauld JC. Interleukin-22 (IL-22) activates the JAK/STAT, ERK, JNK, and p38 MAP kinase pathways in a rat hepatoma cell line. Pathways that are shared with and distinct from IL-10. J Biol Chem. 2002; 277:33676–82. [PubMed: 12087100]

Liang SC, Tan XY, Luxenberg DP, Karim R, Dunussi-Joannopoulos K, Collins M, et al. Interleukin (IL)-22 and IL-17 are coexpressed by Th17 cells and cooperatively enhance expression of antimicrobial peptides. J Exp Med. 2006; 203:2271–9. [PubMed: 16982811]

Liu S, Xu SW, Blumbach K, Eastwood M, Denton CP, Eckes B, et al. Expression of integrin beta1 by fibroblasts is required for tissue repair in vivo. J Cell Sci. 2010; 123:3674–82. [PubMed: 20940256]

Lowes MA, Kikuchi T, Fuentes-Duculan J, Cardinale I, Zaba LC, Haider AS, et al. Psoriasis vulgaris lesions contain discrete populations of Th1 and Th17 T cells. J Invest Dermatol. 2008; 128:1207–11. [PubMed: 18200064]

Ma HL, Liang S, Li J, Napierata L, Brown T, Benoit S, et al. IL-22 is required for Th17 cell-mediated pathology in a mouse model of psoriasis-like skin inflammation. J Clin Invest. 2008; 118:597–607. [PubMed: 18202747]

Martin B, Hirota K, Cua DJ, Stockinger B, Veldhoen M. Interleukin-17-producing gammadelta T cells selectively expand in response to pathogen products and environmental signals. Immunity. 2009; 31:321–30. [PubMed: 19682928]

Montesano R, Orci L. Transforming growth factor beta stimulates collagen-matrix contraction by fibroblasts: implications for wound healing. Proc Natl Acad Sci U S A. 1988; 85:4894–7. [PubMed: 3164478]

O'Connor W, Kamanaka M, Booth CJ, Town T, Nakae S, Iwakura Y, et al. A protective function for interleukin 17A in T cell-mediated intestinal inflammation. Nat Immunol. 2009; 10:603–9. [PubMed: 19448631]

Qiu C, Coutinho P, Frank S, Franke S, Law LY, Martin P, et al. Targeting connexin43 expression accelerates the rate of wound repair. Curr Biol. 2003; 13:1697–703. [PubMed: 14521835]

Radaeva S, Sun R, Pan HN, Hong F, Gao B. Interleukin 22 (IL-22) plays a protective role in T cell-mediated murine hepatitis: IL-22 is a survival factor for hepatocytes via STAT3 activation. Hepatology. 2004; 39:1332–42. [PubMed: 15122762]

Sasaki JR, Zhang Q, Schwacha MG. Burn induces a Th-17 inflammatory response at the injury site. Burns. 2011; 37:646–51. [PubMed: 21353393]

Sawicki G, Marcoux Y, Sarkhosh K, Tredget EE, Ghahary A. Interaction of keratinocytes and fibroblasts modulates the expression of matrix metalloproteinases-2 and -9 and their inhibitors. Mol Cell Biochem. 2005; 269:209–16. [PubMed: 15786734]

Sekikawa A, Fukui H, Suzuki K, Karibe T, Fujii S, Ichikawa K, et al. Involvement of the IL-22/REG Ialpha axis in ulcerative colitis. Lab Invest. 2010; 90:496–505. [PubMed: 20065946]

Snyder M, Huang XY, Zhang JJ. Identification of novel direct Stat3 target genes for control of growth and differentiation. J Biol Chem. 2008; 283:3791–8. [PubMed: 18065416]

Steenvoorden MM, Tolboom TC, van der Pluijm G, Löwik C, Visser CP, DeGroot J, et al. Transition of healthy to diseased synovial tissue in rheumatoid arthritis is associated with gain of mesenchymal/fibrotic characteristics. Arthritis Res Ther. 2006; 8:R165. [PubMed: 17076892]

Takatori H, Kanno Y, Watford WT, Tato CM, Weiss G, Ivanov II, et al. Lymphoid tissue inducer-like cells are an innate source of IL-17 and IL-22. J Exp Med. 2009; 206:35–41. [PubMed: 19114665]

Tammela T, Zarkada G, Wallgard E, Murtomäki A, Suchting S, Wirzenius M, et al. Blocking VEGFR-3 suppresses angiogenic sprouting and vascular network formation. Nature. 2008; 454:656–60. [PubMed: 18594512]

Truchetet ME, Brembilla NC, Montanari E, Allanore Y, Chizzolini C. Increased frequency of circulating Th22 in addition to Th17 and Th2 lymphocytes in systemic sclerosis: association with interstitial lung disease. Arthritis Res Ther. 2011; 13:R166. [PubMed: 21996293]

Tumbar T, Guasch G, Greco V, Blanpain C, Lowry WE, Rendl M, et al. Defining the epithelial stem cell niche in skin. Science. 2004; 303:359–63. [PubMed: 14671312]

Valenzuela DM, Murphy AJ, Frendewey D, Gale NW, Economides AN, Auerbach W, et al. High-throughput engineering of the mouse genome coupled with high-resolution expression analysis. Nat Biotechnol. 2003; 21:652–9. [PubMed: 12730667]

Van Vliet E, Melis M, Van Ewijk W. Monoclonal antibodies to stromal cell types of the mouse thymus. Eur J Immunol. 1984; 14:524–9. [PubMed: 6734714]

Werner S, Grose R. Regulation of wound healing by growth factors and cytokines. Physiol Rev. 2003; 83:835–70. [PubMed: 12843410]

Wolk K, Kunz S, Witte E, Friedrich M, Asadullah K, Sabat R. IL-22 increases the innate immunity of tissues. Immunity. 2004; 21:241–54. [PubMed: 15308104]

Wolk K, Witte E, Wallace E, Döcke WD, Kunz S, Asadullah K, et al. IL-22 regulates the expression of genes responsible for antimicrobial defense, cellular differentiation, and mobility in

keratinocytes: a potential role in psoriasis. Eur J Immunol. 2006; 36:1309–23. [PubMed: 16619290]

Xie MH, Aggarwal S, Ho WH, Foster J, Zhang Z, Stinson J, et al. Interleukin (IL)-22, a novel human cytokine that signals through the interferon receptor-related proteins CRF2–4 and IL-22R. J Biol Chem. 2000; 275:31335–9. [PubMed: 10875937]

Yamamoto-Furusho JK, Miranda-Pérez E, Fonseca-Camarillo G, Sánchez-Muñoz F, Dominguez-Lopez A, Barreto-Zuñiga R. Colonic epithelial upregulation of interleukin 22 (IL-22) in patients with ulcerative colitis. Inflamm Bowel Dis. 2010; 16:1823. [PubMed: 20222141]

Zenewicz LA, Yancopoulos GD, Valenzuela DM, Murphy AJ, Karow M, Flavell RA. Interleukin-22 but not interleukin-17 provides protection to hepatocytes during acute liver inflammation. Immunity. 2007; 27:647–59. [PubMed: 17919941]

Zenewicz LA, Yancopoulos GD, Valenzuela DM, Murphy AJ, Stevens S, Flavell RA. Innate and adaptive interleukin-22 protects mice from inflammatory bowel disease. Immunity. 2008; 29:947–57. [PubMed: 19100701]

Zhang W, Dang E, Shi X, Jin L, Feng Z, Hu L, et al. The Pro-Inflammatory Cytokine IL-22 Up-Regulates Keratin 17 Expression in Keratinocytes via STAT3 and ERK1/2. PLoS One. 2012; 7:e40797. [PubMed: 22808266]

Zheng Y, Danilenko DM, Valdez P, Kasman I, Eastham-Anderson J, Wu J, et al. Interleukin-22, a T(H)17 cytokine, mediates IL-23-induced dermal inflammation and acanthosis. Nature. 2007; 445:648–51. [PubMed: 17187052]
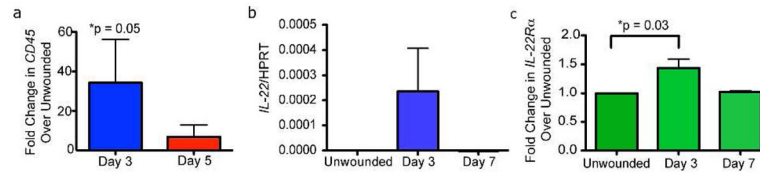
Figure 1. *IL-22* mRNA Is Expressed During Acute Skin Wounding
CD45 (A), *IL-22* (B) and *IL-22Rα* (C) mRNA expression via Real Time PCR in unwounded skin or wounds of mice after indicated timepoints. n= 3 wounds from 3 mice for each timepoint. All data are ± SEM. Asterisks indicate significance.
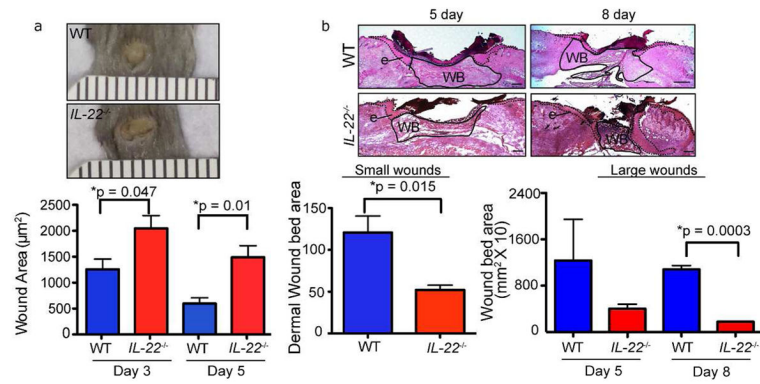
Figure 2. *IL-22*$^{-/-}$ mice exhibit defects in the dermis during wound healing
A) Images of WT and *IL-22*$^{-/-}$ backskin 3 days after wounding with 2mm punch biopsies. Quantification of the external area of WT and *IL-22*$^{-/-}$ small wounds at 3 and 5 days post-wounding. n>18 wounds for each genotype (6 wounds from 6 mice for each of 3 independent experiments). Ruler notches=1mm. B) Hematoxylin and eosin stained sections of WT and *IL-22*$^{-/-}$ backskins wounded with 8mm punch biopsies (large wounds). Epidermis (e) is indicated by dotted line and wound bed (WB) is outlined by solid line. Quantification of wound bed area (i.e. dermal area) of small wounds (2mm) 3 days post wounding and large wounds (8mm) 5 and 8 days post wounding in WT and *IL-22*$^{-/-}$ mice are shown. For small wounds, n = 18 (6 wounds from 6 mice for each of 3 independent experiments). For large wounds, n= 12 wounds from 6 mice. Bars = 400μm. All data are ± SEM. Asterisks indicate significance.
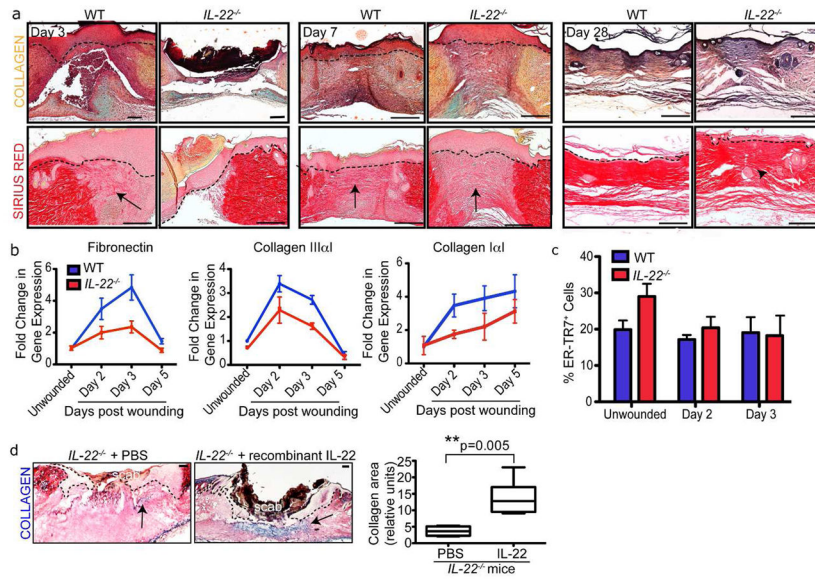
Figure 3. *IL-22^{−/−}* mice exhibit defects in extracellular matrix production

A) Skin sections of WT and *IL-22^{−/−}* mice 3, 7 and 28 days post wounding with 2mm punch biopsies were stained with Movat Pentachrome (collagen, yellow; mucin, blue) and Sirius Red (Collagen Type III, red). Bars = 200 μm. Arrows indicate collagen, arrowhead indicates disorganized collagen. B) Real Time PCR analysis reveals decreased Fibronectin, Collagen IaI and Collagen IIIaI mRNA levels in 2mm IL-22^{−/−} skin wounds. n= 4 mice for each genotype and timepoint. C) Quantification of % ER-TR7+ cells in the total dermal cell population derived from the dermis of WT and *IL-22^{−/−}* mice wounded with 2mm punch biopsies. n=4 mice for each genotype. D) Skin sections of *IL-22^{−/−}* skin 5 days post-wounding that were injected with PBS or recombinant IL-22 on day 3 and stained with trichrome histological stain (collagen, blue). Bars = 200 μm. Quantification of the area of collagen in the wound beds of *IL-22^{−/−}* mice injected with PBS or 25ng recombinant IL-22. n= 6 mice. Asterisks indicate significance. All data are mean +/− SEM.
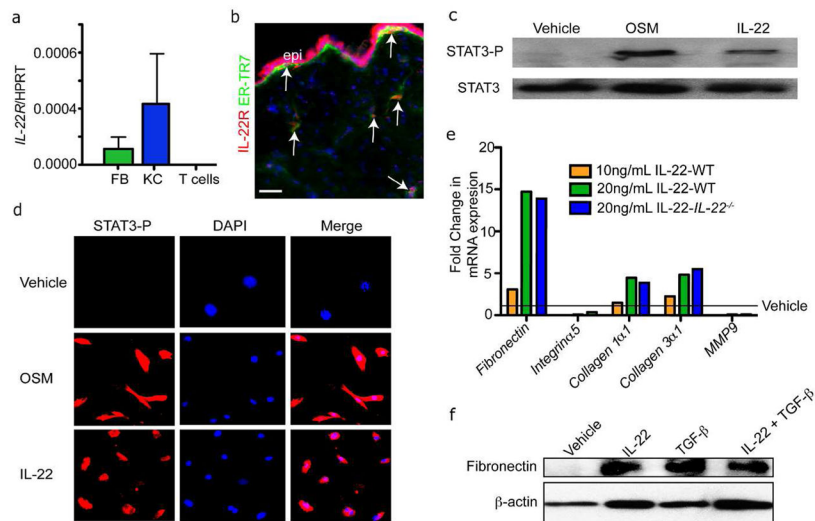
Figure 4. IL-22 can stimulate STAT3 activation and ECM production in dermal fibroblasts
A) Real time PCR reveals that isolated dermal fibroblasts (FB) and keratinocytes (KC)
express *IL-22Rα* mRNA. n=3 mice. Data are mean +/− SEM. B) Skin sections of were
immunostained with antibodies against IL-22Rα and ER-TR7. Arrows indicate ER-TR7+
and IL-22Rα^Ecells. Bar = 100 μm. epi, epidermis. C) Representative images of primary
mouse fibroblasts immunostained with antibodies against phospho-STAT3 (STAT3-P) after
treated with IL-22 or oncostatin M (OSM) for 20 minutes. D) Western blot analysis
confirms the increased activation of STAT3-P in primary dermal fibroblasts treated with
IL-22 or Oncostatin M. E) Real time PCR analysis of mRNA in WT or *IL-22*$^{-/-}$ primary
mouse fibroblasts reveals enhanced expression of ECM genes after IL-22 stimulation for 48
hours. F) Western blot analysis shows that IL-22 increases the expression of fibronectin
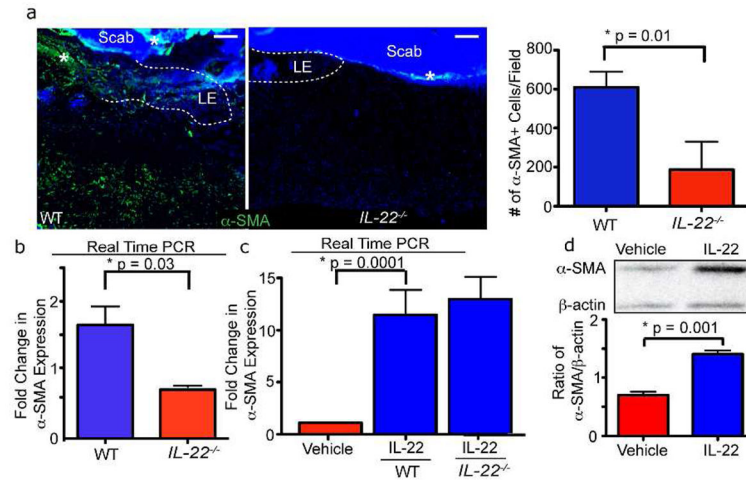protein in WT fibroblasts. *β-actin* is included as a loading control.

Figure 5. IL-22 induces myofibroblast differentiation
A) Skin sections of WT and *IL-22*$^{-/-}$ mice 3 days after wounding with 2mm punch biopsies were immunostained with antibodies against α-SMA. Quantification of α-SMA staining, n = 6 mice for each genotype. B) Real time PCR reveals reduced mRNA expression of α-SMA in 2mm *IL-22*$^{-/-}$ wounds 3 days post-wounding. n= 4 mice for each genotype and each timepoint. C) Real time PCR analysis of WT or *IL-22*$^{-/-}$ primary dermal fibroblasts cultured with vehicle or recombinant IL-22 for 48 hours confirms that *α-SMA* mRNA expression increases with IL-22 stimulation. n = 3 independent experiments. D) α-SMA protein expression increases in primary fibroblasts after stimulation with IL-22 for 48 hours as indicated by representative image of western analysis. Quantification of the ratio of α-SMA/β-actin expression is shown. n = 3 independent experiments. All data are mean +/− SEM.